QUANTIFYING THE RESPONSE OF BLAINVILLE'S BEAKED WHALES TO U.S. NAVAL SONAR EXERCISES IN HAWAII

Eiren K. Jacobson[1]*, E. Elizabeth Henderson[2], Cornelia S. Oedekoven[1], David L. Miller[1], Stephanie L. Watwood[3], David J. Moretti[3], Len Thomas[1]

[1] *Centre for Research into Ecological and Environmental Modelling, University of St Andrews, St Andrews, Scotland, UK*

[2] *Naval Information Warfare Center Pacific, San Diego, CA, USA*

[3] *Naval Undersea Warfare Center, Newport, RI, USA*

Corresponding author (email: eiren.jacobson@st-andrews.ac.uk)

Draft 17 January 2020

Abstract

Naval use of mid-frequency active (MFA) sonar has been associated with injury and death of multiple species of marine mammals. Deep-diving beaked whales (family Ziphiidae) are particularly susceptible to naval sonar. The US Navy operates multiple training and testing facilities where MFA sonar is used regularly, and where cumulative sublethal impacts of exposure to MFA sonar could have negative effects on beaked whale populations. Responses of beaked whales to MFA sonar have been quantified in the form of risk functions for some species and regions. Our goal was to develop a risk function for Blainville's beaked whales *(Mesoplodon densirostris)* on the Pacific Missile Range Facility (PMRF) in Hawaii and to compare our risk function to another developed for the same species in a different ocean basin. We used passive acoustic data collected at bottom-mounted hydrophones before and during six Naval training exercises at PMRF in conjunction with modelled sonar received levels to describe the effect of Naval training and Naval MFA sonar on foraging groups of Blainville's beaked whales. We used a multi-stage generalized additive modelling (GAM) approach . . .

We found that . . .

---

1 Introduction

Beaked whales (family Ziphiidae) are a group of deep-diving cetaceans that rely on sound to forage, navigate, and communicate (Aguilar de Soto et al., 2012; Johnson, Madsen, Zimmer,

Aguilar de Soto, and Tyack, 2004; Macleod and D'Amico, 2006). Multiple mass strandings of beaked whales have been associated with high-intensity anthropogenic sound sources. These acute events have motivated research into whether and how beaked whales respond to different types and intensities of anthropogenic noise (Cox et al., 2006).

Anthropogenic sound can disrupt the patterned dive cycles of beaked whales [CITE e.g. Falcone, also Southall re syncrhronicity?], potentially leading to death [CITE Jepson] or to cumulative sublethal impacts [PCoD, CITE]. For example, research on Blainville's beaked whales *Mesoplodon densirostris* on a Navy range in the Bahamas has shown that animals may stop foraging and/or move away from Naval sonar sources (Joyce et al., 2019; Tyack et al., 2011).

Naval sonar can be broadcast from various platforms, including vessels, helicopters, buoys, submarines, and torpedoes (Harris et al., 2019; Navy, 2018). Most research has focused on the impacts of mid-frequency active (MFA) sonar broadcast from US Naval vessels, but has not been able to isolate the effect of associated training activity beyond MFA sonar. Separately, researchers have shown that, in the absence of MFA sonar, beaked whales may alter their behavior in response to vessel noise (Aguilar Soto et al., 2006; Pirotta et al., 2012).

There are different experimental and analytical ways of quantifying responses to sonar. Here, we focus on methods used for analysis of data from cabled hydrophone arrays.

For example, (McCarthy et al., 2011) used separate generalized additive models (GAMs) for before/during/after, response was GVPs per 5 hr periods, explanatory vars were inner/outer and time. Hypotheses were evaluated using z-tests.

(Moretti et al., 2014) used a GAM to model the presence or absence of acoustic detections of groups of Blainville's beaked whales on the AUTEC range as a function of a smooth on MFA sonar received level. They then compared . . . probability of disturbance. They found that fograging dive behavior was reduced by 50% at 150 dbrms re 1μPa.

In the present study, our primary objective was to replicate the effort of Moretti et al. with the same species on a different US Navy training range in a different oceanic environment. Unlike AUTEC, which occurs in a deep isolated basin surrounded by steep slopes, the Pacific Missile Range Facility (PMRF) range occurs on the side of an ancient volcano, with a steep slope down to the deep ocean floor. Density is lower and more variable, so we wanted to explicitly accounting for differences in underlying beaked whale presence.

In addition, a secondary objective was to examine the cumulative effects of Naval training activity and MFA sonar while We wanted to isolate the effect of training activity from the effect of hull-mounted MFA sonar.

To accomplish these objectives, we used a spatially referenced dataset of Blainville's beaked whale foraging dives recorded off the island of Kauai, Hawaii. Acoustic detections of Blainville's beaked whales were collected via a cabled hydrophone array at PMRF before and during six Naval training exercises. Previous work in this region has shown that Blainville's beaked whales are present year-round at this site, that they prefer certain slope habitats, and that acoustic detections decrease during multi-day training events (Henderson, Martin, Manzano-Roth, and Matsuyama, 2016; Manzano-Roth, Henderson, Martin, Martin, and Matsuyama,

2016).

Summary here of methods.

2 Methods

2.1 Acoustic detection of beaked whales

The Pacific Missile Range Facility (PMRF) is an instrumented U.S. Naval range extending 70 km NW of the island of Kauai, Hawaii and encompassing 2,800 km^2. The range includes a cabled hydrophone array (Fig. 1) with hydrophones at depths ranging from approximately 650 m to 4,700 m. Hydrophones had a sample rate of 96 kHz, with the high pass filter on each phone set at either 50 Hz, 100 Hz, or 10 kHz. Up to 62 of the range hydrophones at a time can be recorded simultaneously by the Naval Information Warfare Center (NIWC). The Navy Acoustic Range WHale AnaLysis (NARWHAL) algorithm suite includes a Blainville's beaked whale detector that first compares signal-to-noise (SNR) thresholds within the expected beaked whale click frequency range (16 - 44 kHz) versus the bandwidth outside the click in a running 16384-pt fast Fourier transform (FFT) spectrogram. The detected clicks are then passed to a 64-pt FFT stage that measures power, bandwidth, slope, and duration characteristics to classify the clicks to species. This process is followed by an automated routine in Matlab (CITE Mathworks 2019) used to group detections of individual beaked whale echolocation clicks into Group Vocal Periods (GVPs). If a group of whales is detected by more than one hydrophone, the GVP is assigned to the hydrophone that recorded the most clicks. The data are then aggregated to indicate the presence or absence of the start of a GVP for each hydrophone within each half-hour period. In the present study, we used data collected before and during Submarine Commander Courses (SCCs) at the PMRF. SCCs occur biannually in February and August. SCCs typically last 6-7 days, and the period before the onset of the SCC is recorded for a minimum of 2 days.

2.2 Modelling received levels of hull-mounted mid-frequency active sonar

Classified ship positional data and other activity that occurs on the range during each SCC are provided by PMRF. This data indicate the locations of the ships during the training periods and also indicate the start and stop times of each individual training event, but no information is provided on the start and stop of sonar use. Periods of active sonar are determined by running the sonar detector tuned to mid-frequency active (MFA) sonar, as part of the NARWHAL algorithm suite. Using these data, the locations of all surface ships are noted for each half-hour period and the closest ship to each hydrophone is determined. Propagation modelling is used to calculate the expected received level of hull-mounted mid-frequency active sonar at the location of each hydrophone from the closest ship during each half-hour period of each SCC. The propagation modelling is done using the parabolic

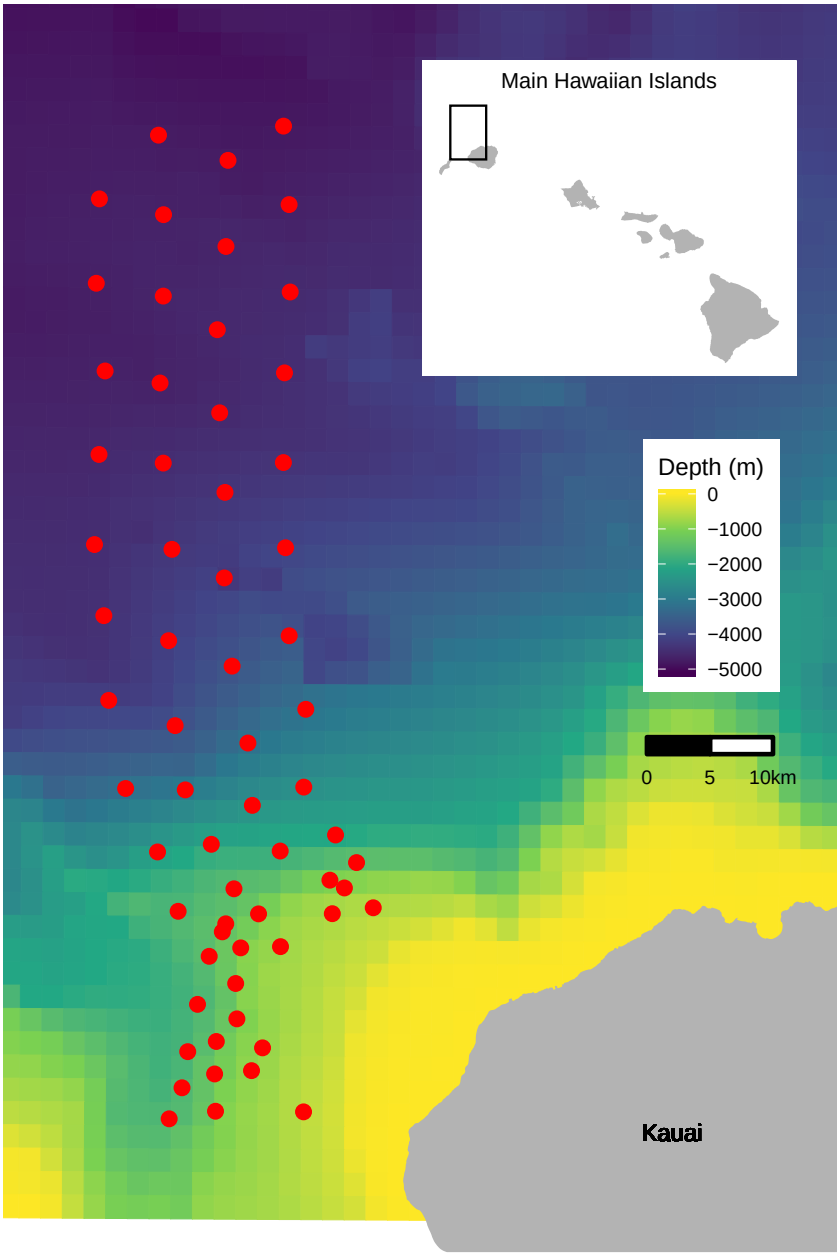

Figure 1: Map of approximate locations of hydrophones (red points) at the Pacific Missile Range Facility. Inset map shows range location relative to the Main Hawaiian Islands.

equation propagation model in the program Peregrine (OASIS; Heaney and Campbell, 2016) to estimate the transmission loss between the ship and the hydrophone; this was then converted to a received level at the hydrophone location based on the source level of the sonar. However, if the distance between the ship and the hydrophone was less than the depth of the water column, the parabolic equation overestimates transmission loss at that angle and so a simple sonar equation was used to estimate transmission loss instead. Transmission loss is estimated using a 200 Hz band around the center frequency of the sonar type (here, 3.5 kHz). Transmission loss is estimated at depth since Blainville's beaked whales don't begin clicking until they have reached approximately XX m depth of their foraging dive and spend most of their foraging dive at around 1000 m (REF). For hydrophones shallower than 1000 m the received level is estimated at a point 20 m above the sea floor with a +/- 10 m buffer, while for hydrophones deeper than 1000 m the received level is estimated at 1000 m depth with a +/- 10 m buffer. The location of the beaked whale foraging group is assumed to be within 4-6 km of the hydrophone with the most click detections, as beaked whale echolocation clicks attenuate beyond that distance (T. A. Marques, Thomas, Ward, DiMarzio, and Tyack, 2009; McCarthy et al., 2011). Therefore the transmission loss is estimated along the radial from the ship to the hydrophone from a distance of 1 km before the hydrophone to 1 km past the hydrophone in 200 m increments. The maximum modeled received level along that radial was determined for each hydrophone and half-hour period and aggregated with the data on beaked whale group detections. Uncertainty in the modelled received level was not considered.

2.3 Spatial Modelling

Modelling methods are described in detail in the following sections. Briefly, we first used a tesselation to determine the area effectively monitored by each hydrophone. Then, we used pre-activity data to create a spatial model of the probability of GVPs prior to the onset of Naval activity. We used the predicted values from this model as an offset in a model created using data from when Naval activity was present on the range, but MFA sonar was not. Again, we used the predicted values from this model as an offset in a model created using data when Naval activity and MFA sonar were present on the range. Finally, we used posterior simulation to calculate confidence intervals and quantified the change in the probability of GVPs when Naval activity was present and across received levels of MFA sonar.

2.3.1 Determining hydrophone effort

For security reasons, randomly "jittered" locations and depths of hydrophones at PMRF were used. We projected the coordinates of each hydrophone into Universal Transverse Mercator Zone 4.

Because the beaked whale detection algorithm assigns groups of whales to the hydrophone that recorded the most echolocation clicks, and because the spatial separation of the hydrophones is not uniform, effort is not the same for all hydrophones. To determine the area effectively

monitored by each hydrophone, we used a Voronoi tesselation implemented in the R (R Core Team, 2018) package `deldir` (Turner, 2019) to define a tile for each hydrophone that contained all points on the range that were closest to that hydrophone. The area of each tile corresponds to the effective area monitored. We assume that beaked whale groups occur within the tesselation tile of the hydrophone to which the GVP is assigned. For hydrophones on the outside of the range, i.e., not surrounded by other hydrophones, we used a cutoff radius of 6500 m to bound the tesselation tile. This distance is based on the maximum detection distance of individual Blainville's beaked whale clicks at a U.S. Naval range in the Bahamas (T. A. Marques et al., 2009). Different combinations of hydrophones were used during different SCCs, so separate tesselations were created for each SCC.

2.3.2 M1: Modelling the pre-activity probability of dive detection

We used data collected prior to SCCs, when no Naval ships were present on the range and no other Naval activity was known to occur, to determine the baseline probability of GVPs at each hydrophone. The exact locations of beaked whale groups is not known; rather, detections of beaked whale groups are "snapped" to hydrophone locations depending on which hydrophone detected the most echolocation clicks. Therefore, the data are not continuous in space. To account for this, we used a Markov random field to model the spatial distribution of GVPs. A Markov random field (Rue and Held, 2005) is a method for modelling correlation in space between discrete spatial units. Each unit is correlated more strongly with its neighbours (those units which touch) than those that are more hops away. This gives a graph-like structure, where "number of hops" is the distance used to calculate relatedness, rather than geographical distance. This is appropriate for our data as we do not know where in each tile a given GVP occurs, but we assume that it does occur in that tile.

The R package `mgcv` (Wood, Li, Shaddick, and Augustin, 2017) was used to formulate the model on the tesselation described in the previous section. The linear predictor for the model was:

$$\text{logit}\left(\mu_{\texttt{M1},i}\right) = \beta_{\texttt{M1},0} + f(\texttt{MRF}_i) + f(\texttt{Depth}_i) + \log_e A_i, \qquad (\texttt{M1}) \tag{1}$$

where $\texttt{DivePresent}_i \sim \text{Bin}(1,_{\texttt{M1},i})$. The spatial smooth MRF is given by $f(\texttt{MRF}_i)$, $f(\texttt{Depth}_i)$ is a smooth of depth (using a thin plate spline) and $\log_e A_i$ is an offset for the area (in km^2) of each tile, A_i. The offset term accounts changes in probabilities of detection due to the differing area monitored per hydrophones. Because the hydrophone tesselations change between SCCs, separate MRFs were used for each SCC, but a single smoothing parameter was estimated across all MRFs. Therefore different spatial patterns could occur, but with the same amount of variation. The smooth of depth was shared across SCCs.

NOTE: f(MRF) could be indexed by SCC to indicate that the smooth function is different for each.

2.3.3 M2: Modelling the effect of Naval activity

For a few days prior to the onset of hull-mounted MFA sonar used during SCCs, other Naval training activities occur at the PMRF. Various vessels are present on the range during this period and other noise sources, including torpedoes and submarines, may be present. We used data collected when training activity was present on the range, but hull-mounted MFA sonar was not used, to model the effect of general Naval activity on beaked whale GVPs. Initially, we tried to use low-frequency noise levels in the 10-999 Hz range measured on range hydrophones as a covariate in this model, but found that the measured noise levels were not consistent with known locations of Naval training activities (see Appendix B for details).

We used the predicted baseline probability of a GVP from Model 1 as an offset to control for the underlying spatial distribution of GVPs. The model for the data when ships were present was intercept-only, with an offset derived from `M1`. This model was simply:

$$\text{logit}\left(\mu_{\texttt{M2},i}\right) = \beta_{\texttt{M2},0} + \log_e \xi_{\texttt{M1},i}, \qquad (\texttt{M2}) \tag{2}$$

where $\texttt{DivePresent}_i \sim \text{Bin}(1, \mu_{\texttt{M2},i})$. $\xi_{\texttt{M1},i}$ denotes the prediction (on the logit scale) for tile i using model `M1`. This was again modelled in the R package `mgcv`.

2.3.4 M3: Modelling the effect of hull-mounted MFA sonar

We used data collected when hull-mounted MFA sonar was present on the range to model the effect of sonar on beaked whales. The probability of a dive when sonar was present was modelled as a function of the maximum received level (modelled at each hydrophone; see section 2.2). We assumed that as the maximum received level increased, the probability of dives decreased and modelled this using a shape constrained smooth so that the relationship held for all possible realizations of the smooth. To ensure that the model predictions were the same at a maximum received level of 0 dB and when ships were not present, we did not include an intercept. This model was written as:

$$\text{logit}\left(\mu_{\texttt{M3},i}\right) = f(\texttt{MaxRL}_i) + \log_e \xi_{\texttt{M2},i}, \qquad (\texttt{M3}) \tag{3}$$

where $\texttt{DivePresent}_i \sim \text{Bin}(1, \mu_{\texttt{M3},i})$. $f(\texttt{MaxRL}_i)$ was modelled as a monotonic decreasing smooth using the R package `scam` (Pya and Wood, 2015). $\xi_{\texttt{M2},i}$ denotes the prediction (on the logit scale) for tile i when Naval training activites were present on the range using model `M2`.

2.3.5 Uncertainty propagation

We used posterior simulation to propagate uncertainty through M1, M2, and M3. Each model was fitted via restricted maximum likelihood (REML; Wood, 2008), so the results are empirical Bayes estimates. In this case we can generate samples from the (multivariate normal) posterior of the model parameters. After generating a sample, $\boldsymbol{\beta}^* \sim \text{MVN}(\hat{\boldsymbol{\beta}}, \mathbf{V}_\beta)$,

we can use the matrix that maps the model parameters to the predictions on the linear predictor scale [often referred to as the $\mathbf{L}_p$ matrix or $\mathbf{X}_p$ matrix; Wood et al. (2017); section 7.2.6], along with the inverse link function to generate predictions for each posterior sample. Here the $\boldsymbol{\beta}$ for each model includes the coefficients for the smooth terms in the model and fixed effects (e.g., intercept) if present. Predictions, $\boldsymbol{\mu}^*$, can be written as:

$$\boldsymbol{\mu}^* = g^{-1}(\eta^*) = g^{-1}(\mathbf{X}_p\boldsymbol{\beta}^* + \boldsymbol{\xi}), \tag{4}$$

where g is the link function, η^* is the linear predictor and $\boldsymbol{\xi}$ is any offset used by this prediction. By sampling from the posterior of $\hat{\boldsymbol{\beta}}$, and then taking the variance of the resulting $\mathbf{p}^*$s we can obtain variance estimates [Wood et al. (2017); section 7.2.6]. The prediction grid contained all possible combinations of covariates within the realized covariate space; i.e., each hydrophone for each SCC with associated location, hydrophone depth, and area of the tesselation tile, presence/absence of Naval activity, and, if Naval activity present, then either sonar absence or sonar received level between 35 and 190 dB in intervals of 5 dB.

This procedure needs to happen for each model, updating the offsets and refitting as it goes.

An algorithm for calculating the variance from our multi-stage approach is as follows. First define N_b as the number of samples to make, let $\mathbf{X}_{p,\mathtt{M}j}$ for $j = 1, 2, 3$ be the $\mathbf{L}_p$ matrix that maps coefficients to the predictions for model $\mathtt{M}j$. For N_b times:

1. Draw a sample from the posterior of $\mathtt{M1}$: $\tilde{\boldsymbol{\beta}}_{\mathtt{M1}} \sim \text{MVN}(\hat{\boldsymbol{\beta}}_{\mathtt{M1}}, \mathbf{V}_{\mathtt{M1}})$.
2. Calculate a new offset for $\mathtt{M2}$, $\tilde{\boldsymbol{\xi}}_{\mathtt{M1}} = \mathbf{X}_{p,\mathtt{M1}}\tilde{\boldsymbol{\beta}}_{\mathtt{M1}} + \log_e \mathbf{A}$.
3. Refit $\mathtt{M2}$ with $\tilde{\boldsymbol{\xi}}_{\mathtt{M1}}$ as the offset, to obtain $\mathtt{M2}'$.
4. Draw a sample from the posterior of $\mathtt{M2}'$: $\tilde{\boldsymbol{\beta}}_{\mathtt{M2}'} \sim \text{MVN}(\hat{\boldsymbol{\beta}}_{\mathtt{M2}'}, \mathbf{V}_{\mathtt{M2}'})$
5. Calculate a new offset for $\mathtt{M3}$, $\tilde{\boldsymbol{\xi}}_{\mathtt{M2}} = \mathbf{X}_{p,\mathtt{M2}}\tilde{\boldsymbol{\beta}}'_{\mathtt{M2}} + \tilde{\boldsymbol{\xi}}_{\mathtt{M1}}$ (predictions for the sonar data locations for $\mathtt{M2}'$).
6. Refit $\mathtt{M3}$ with offset $\tilde{\boldsymbol{\xi}}_{\mathtt{M2}}$ to obtain $\mathtt{M3}'$.
7. Predict $\boldsymbol{\mu}_{\mathtt{M1}'}$, $\boldsymbol{\mu}_{\mathtt{M2}'}$, and $\boldsymbol{\mu}_{\mathtt{M3}'}$ over prediction grid and store them.

We can then calculate summary statistics (means and variances) of the N_b values of $\boldsymbol{\mu}_{\mathtt{M1}'}$, $\boldsymbol{\mu}_{\mathtt{M2}'}$, and $\boldsymbol{\mu}_{\mathtt{M3}'}$ we have generated. The empirical variance of the N_b values of $\boldsymbol{\mu}_{\mathtt{M3}'}$ will give the uncertainty, incorporating components from all three models. We can take appropriate quantiles to form confidence intervals for the functional relationships between [TKTKTK noisey boi] and [TKTKTK whaley boi].

2.3.6 Quantifying the change in probability of GVPs

Finally, we calculated the expected change in the probability of GVPs relative to either the distribution of GVPs when no general Naval training activity was present and no MFA sonar

was present ($\Delta_{M3':M1'}$), or relative to the distribution of GVPs general Naval training activity was present but no MFA sonar was present ($\Delta_{M3':M2'}$).

Using the N_b bootstrapped model realizations we calculated the expected probability of a GVP under each set of covariates as

$$\mathbb{P}(\text{GVP}) = \text{logit}^{-1}(\mu_{\texttt{M}'}), \tag{5}$$

for each $\texttt{M1}'$, $\texttt{M2}'$, and $\texttt{M3}'$. Then, we calculated the change in $\mathbb{P}(\text{GVP})$ for each set of covariates $\texttt{M3}'$ and $\texttt{M1}'$ ($\Delta_{M3':M1'}$) and between $\texttt{M3}'$ and $\texttt{M2}'$ ($\Delta_{M3':M2'}$) for each realization of the bootstrap.

$$\Delta_{M3':M1'} = \frac{\mathbb{P}(\text{GVP})_{\texttt{M3}'} - \mathbb{P}(\text{GVP})_{\texttt{M1}'}}{\mathbb{P}(\text{GVP})_{\texttt{M1}'}} \tag{6}$$

$$\Delta_{M3':M2'} = \frac{\mathbb{P}(\text{GVP})_{\texttt{M3}'} - \mathbb{P}(\text{GVP})_{\texttt{M2}'}}{\mathbb{P}(\text{GVP})_{\texttt{M2}'}} \tag{7}$$

For each received level we calcualted the 2.5th, 50th, and 97.5th quantiles of $\Delta_{M3':M1'}$ and $\Delta_{M3':M2'}$ to create 95% CIs of change in $\mathbb{P}(\text{GVP})$ across possible received levels. We consider that the probability of disturbance is equal to 1 wherever the 95% CI does not include 0, and 0 otherwise.

3 Results

Data were collected before and during six SCCs; two each in in 2013, 2014, and 2017 (Table 1). The number of hydrophones for which recordings were available varied from 49 to 61. A total of 190928 30-min observations were made.

Table 1: No. of hydrophones used and number of observations made (no. 30-min periods) for each SCC before the exercise began, when Naval activity was present, and when Naval activity and MFA sonar were present.

SCC	HPs	Pre-Activity	Nav. Activity	MFA Sonar
Feb13	61	114	193	124
Aug13	61	209	115	97
Feb14	60	513	111	129
Aug14	61	263	120	128
Feb17	59	450	97	108
Aug17	49	270	106	113

The exact timing of activities during these exercises varied (Fig. 2). For most SCCs, pre-activity data were available immediately preceding the onset of Naval training activity; however, in February 2013 the only available pre-activity data were collected almost a month prior to the onset of Naval training activity. In some SCCs, weekends or other breaks in training resulted in a break in training activity on the range during the days preceding MFA sonar use. MFA sonar was used for 3-4 days during each training event.

Across all SCCs, hydrophones, and conditions, a total of 2312 GVPs were identified. The average probability of a GVP in the dataset was therefore 1%. The spatial distribution of GVPs differed during the pre-activity phases of SCCs (Fig. SX; top panel).

Modelled maximum received levels ranged from 38 to 186 dB re. 1 μ Pa, with a median value when MFA sonar was present of 147 dB re. 1 μ Pa. The intensity and spatial distribution of MFA received levels varied across the range and across SCCs (Fig. SX).

Based on the observed data, the probability of a GVP within a 30-min period changed by -57% when Naval activity was present compared to when Naval activity was absent, by -47% when Naval activity and MFA sonar were present compared to when only ships were present, and by -77% when Naval activity and MFA sonar were present compared to when neither ships nor sonar were present (Fig. S2).

3.2 Results of spatial modelling

We created separate tesselations for each SCC (Fig. SX). In August 2017, data were available from fewer hydrophones, and so in some cases the tesselated tiles, with bounding radius of 6500 m, did not completely cover the range.

Hydrophone depths varied from 648 to 4716 m. The model `M1` predicted highest probability of GVPs at hydrophone depths between 1500 and 2000 m, consistent with other findings that Blainville's beaked whales prefer to forage in slope habitats [CITE].

`M2` used the predicted values from `M1` as an offset and fitted a model to data when Naval activity was ongoing, as indicated by the presence of ships.

- M3 (spline on MaxRL, could reinstate 3-panel figure with dots or line for each HP?)
- Uncertainty prop
- Total change

4 Discussion

- Describe why we didn't use a single giant GAM – didn't want contamination of the baseline period by the spatial distribution of sonar, would lead to underestimates of the impact of sonar. Could present the single giant GAM in an appendix.
- Discuss unusual timeline of Feb13

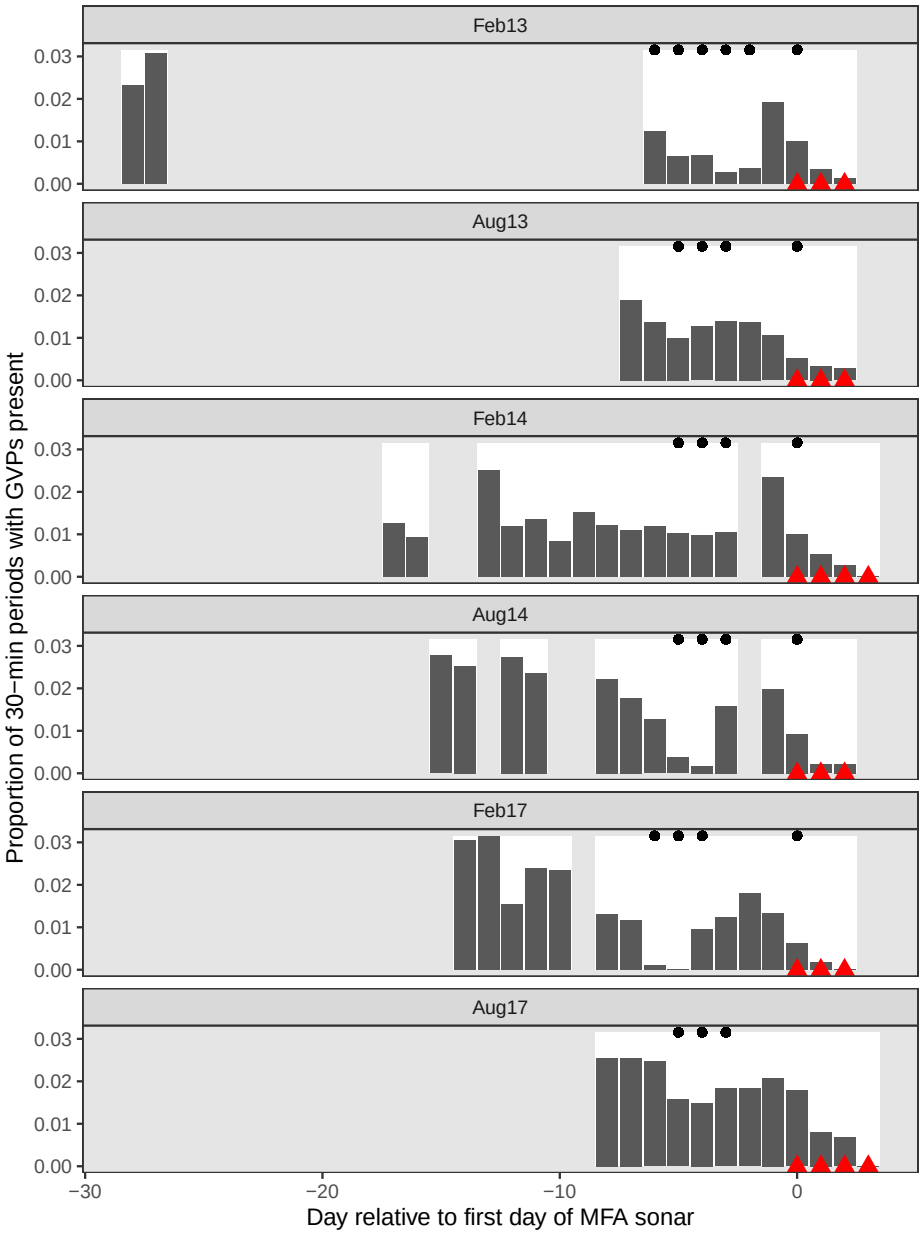

Figure 2: Timeseries of six recorded Naval training activities at PMRF. The timeseries are aligned relative to the first day that MFA sonar (red triangles) was used in each exercise (x-axis). Days with white background indicate days for which recordings and data were available. Gray bars indicate the proportion of 30-min periods on each day, across all hydrophones, when GVPs were detected. Black dots indicate days when Naval activity was present on the range.

- Discuss what "Naval activity" could mean
- GVPs appear to decrease over the course of MFA sonar; this is something we could investigate with a spatio-temporal model in teh future (hour since onset of MFA? SEL?)
- Discuss dose-response and p(disturbance) in context of (Tyack and Thomas, 2019)
- Compare results to Moretti et al 2014; in particular the fact that their "before" was likely actually similar to our "training without sonar"period as it was only 19 hours of data before the onset of sonar and it was the same training scenario as an SCC at PMRF. Therefore our risk function results of the decrease in dives from training without sonar to training with sonar are actually quite similar. Then we can discuss the fact that environment/habitat (e.g. deep basin with shallow slopes all around vs deep open ocean) doesn't seem to play much of a role in Blainville's response, and the response seems to be more of an intrinsic characterisitic. Also can mention here the same effort at SCORE with Cuvier's – in light of these results we expect similar results there even though different species but similar habitat to AUTEC.

References

Aguilar de Soto, N., Madsen, P. T., Tyack, P., Arranz, P., Marrero, J., Fais, A., ... Johnson, M. (2012). No shallow talk: Cryptic strategy in the vocal communication of Blainville's beaked whales. *Marine Mammal Science*, *28*(2), E75–E92. https://doi.org/10.1111/j.1748-7692.2011.00495.x

Aguilar Soto, N., Johnson, M., Madsen, P. T., Tyack, P. L., Bocconcelli, A., & Fabrizio Borsani, J. (2006). DOES INTENSE SHIP NOISE DISRUPT FORAGING IN DEEP-DIVING CUVIER'S BEAKED WHALES (ZIPHIUS CAVIROSTRIS)? *Marine Mammal Science*, *22*(3), 690–699. https://doi.org/10.1111/j.1748-7692.2006.00044.x

Cox, T., Ragen, T., Read, A., Vos, E., Baird, R., Balcomb, K., ... others. (2006). Understanding the impacts of anthropogenic sound on beaked whales1. *J. CETACEAN RES. MANAGE*, *7*(3), 177–187.

Harris, C. M., Martin, S. W., Martin, C., Helble, T. A., Henderson, E. E., Paxton, C. G. M., & Thomas, L. (2019). Changes in the Spatial Distribution of Acoustically Derived Minke Whale (Balaenoptera acutorostrata) Tracks in Response to Navy Training. *Aquatic Mammals*, *45*(6), 661–674. https://doi.org/10.1578/AM.45.6.2019.661

Henderson, E. E., Martin, S. W., Manzano-Roth, R., & Matsuyama, B. M. (2016). Occurrence and Habitat Use of Foraging Blainville's Beaked Whales (Mesoplodon densirostris) on a U.S. Navy Range in Hawaii. *Aquatic Mammals*, *42*(4), 549–562. https://doi.org/10.1578/AM.42.4.2016.549

Johnson, M., Madsen, P. T., Zimmer, W. M. X., Aguilar de Soto, N., & Tyack, P. L. (2004). Beaked whales echolocate on prey. *Proceedings of the Royal Society of London. Series B:*

Biological Sciences, *271*(suppl_6). https://doi.org/10.1098/rsbl.2004.0208

Joyce, T. W., Durban, J. W., Claridge, D. E., Dunn, C. A., Hickmott, L. S., Fearnbach, H., ... Moretti, D. (2019). Behavioral responses of satellite tracked Blainville's beaked whales (*Mesoplodon densirostris*) to mid-frequency active sonar. *Marine Mammal Science*, mms.12624. https://doi.org/10.1111/mms.12624

Macleod, C. D., & D'Amico, A. (2006). *A review of beaked whale behaviour and ecology in relation to assessing and mitigating impacts of anthropogenic noise*. 11.

Manzano-Roth, R., Henderson, E. E., Martin, S. W., Martin, C., & Matsuyama, B. (2016). Impacts of U.S. Navy Training Events on Blainville's Beaked Whale (Mesoplodon densirostris) Foraging Dives in Hawaiian Waters. *Aquatic Mammals*, *42*(4), 507–518. https://doi.org/10.1578/AM.42.4.2016.507

Marques, T. A., Thomas, L., Ward, J., DiMarzio, N., & Tyack, P. L. (2009). Estimating cetacean population density using fixed passive acoustic sensors: An example with Blainville's beaked whales. *The Journal of the Acoustical Society of America*, *125*(4), 1982–1994. https://doi.org/10.1121/1.3089590

McCarthy, E., Moretti, D., Thomas, L., DiMarzio, N., Morrissey, R., Jarvis, S., ... Dilley, A. (2011). Changes in spatial and temporal distribution and vocal behavior of Blainville's beaked whales (Mesoplodon densirostris) during multiship exercises with mid-frequency sonar. *Marine Mammal Science*, *27*(3), E206–E226. https://doi.org/10.1111/j.1748-7692.2010.00457.x

Moretti, D., Thomas, L., Marques, T., Harwood, J., Dilley, A., Neales, B., ... Morrissey, R. (2014). A Risk Function for Behavioral Disruption of Blainville's Beaked Whales (Mesoplodon densirostris) from Mid-Frequency Active Sonar. *PLoS ONE*, *9*(1), e85064. https://doi.org/10.1371/journal.pone.0085064

Navy, U. D. of the. (2018). *Final Environmental Impact Statement/Overseas Environmental Impact Statement Hawaii-Southern California Training and Testing*. Retrieved from https://www.hstteis.com/portals/hstteis/files/hstteis_p3/feis/section/HSTT_FEIS_3.07_Marine_Mammals_October_2018.pdf

Pirotta, E., Milor, R., Quick, N., Moretti, D., Di Marzio, N., Tyack, P., ... Hastie, G. (2012). Vessel Noise Affects Beaked Whale Behavior: Results of a Dedicated Acoustic Response Study. *PLoS ONE*, *7*(8), e42535. https://doi.org/10.1371/journal.pone.0042535

Pya, N., & Wood, S. N. (2015). Shape constrained additive models. *Statistics and Computing*, *25*(3), 543–559. https://doi.org/10.1007/s11222-013-9448-7

R Core Team. (2018). *R: A Language and Environment for Statistical Computing*. Retrieved from https://www.R-project.org/

Rue, H., & Held, L. (2005). *Gaussian Markov Random Fields: Theory and Applications*. London: Chapman & Hall.

Turner, R. (2019). *Deldir: Delaunay Triangulation and Dirichlet (Voronoi) Tessellation*.

Retrieved from https://CRAN.R-project.org/package=deldir

Tyack, P. L., & Thomas, L. (2019). Using dose–response functions to improve calculations of the impact of anthropogenic noise. *Aquatic Conservation: Marine and Freshwater Ecosystems*, *29*(S1), 242–253. https://doi.org/10.1002/aqc.3149

Tyack, P. L., Zimmer, W. M. X., Moretti, D., Southall, B. L., Claridge, D. E., Durban, J. W., ... Boyd, I. L. (2011). Beaked Whales Respond to Simulated and Actual Navy Sonar. *PLoS ONE*, *6*(3), e17009. https://doi.org/10.1371/journal.pone.0017009

Wood, S. N. (2008). Fast stable direct fitting and smoothness selection for generalized additive models. *Journal of the Royal Statistical Society: Series B (Statistical Methodology)*, *70*(3), 495–518.

Wood, S. N., Li, Z., Shaddick, G., & Augustin, N. H. (2017). Generalized Additive Models for Gigadata: Modeling the U.K. Black Smoke Network Daily Data. *Journal of the American Statistical Association*, *112*(519), 1199–1210. https://doi.org/10.1080/01621459.2016.1195744

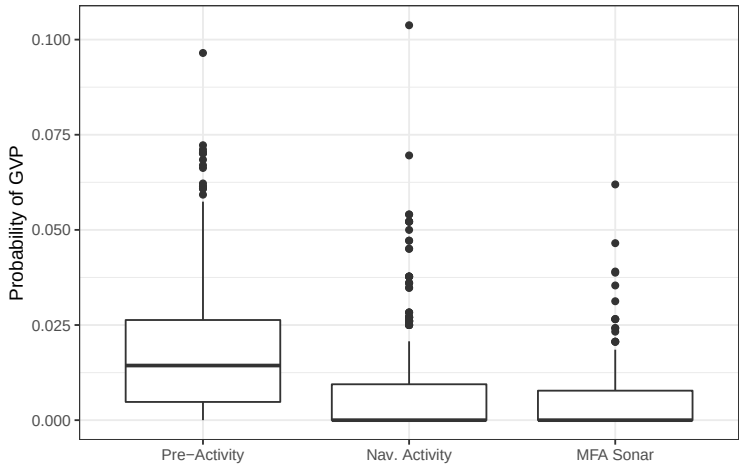

Figure 3: Boxplot of observed probability of diving across all hydrophones and SCCs before, when Naval activity was present, and when MFA sonar was present.

Appendix A: Supplementary Tables and Figures

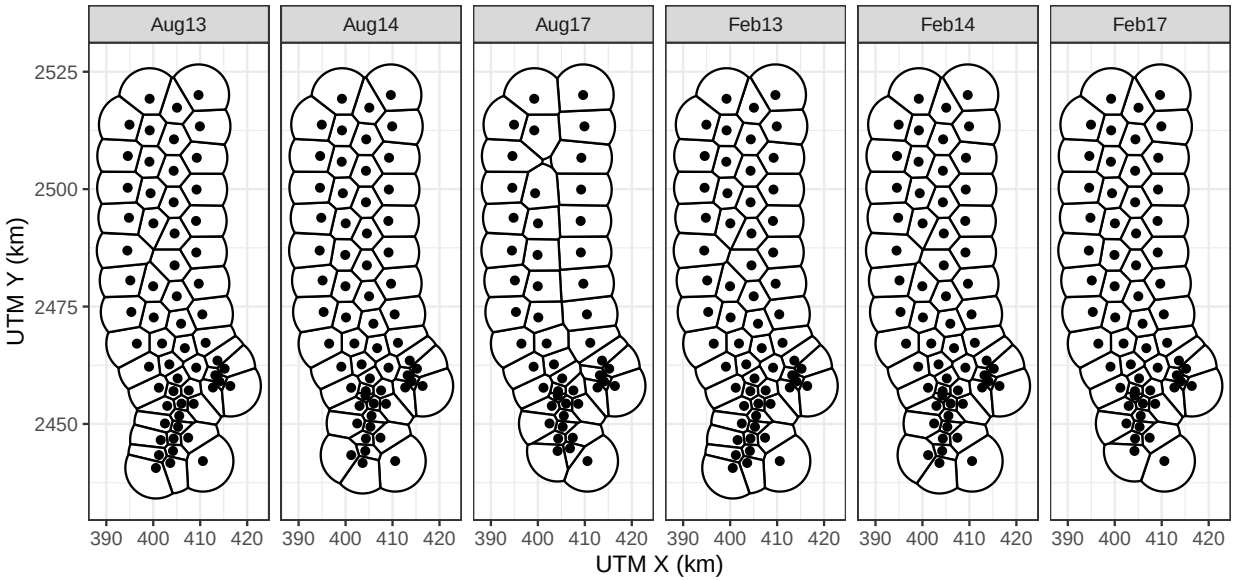

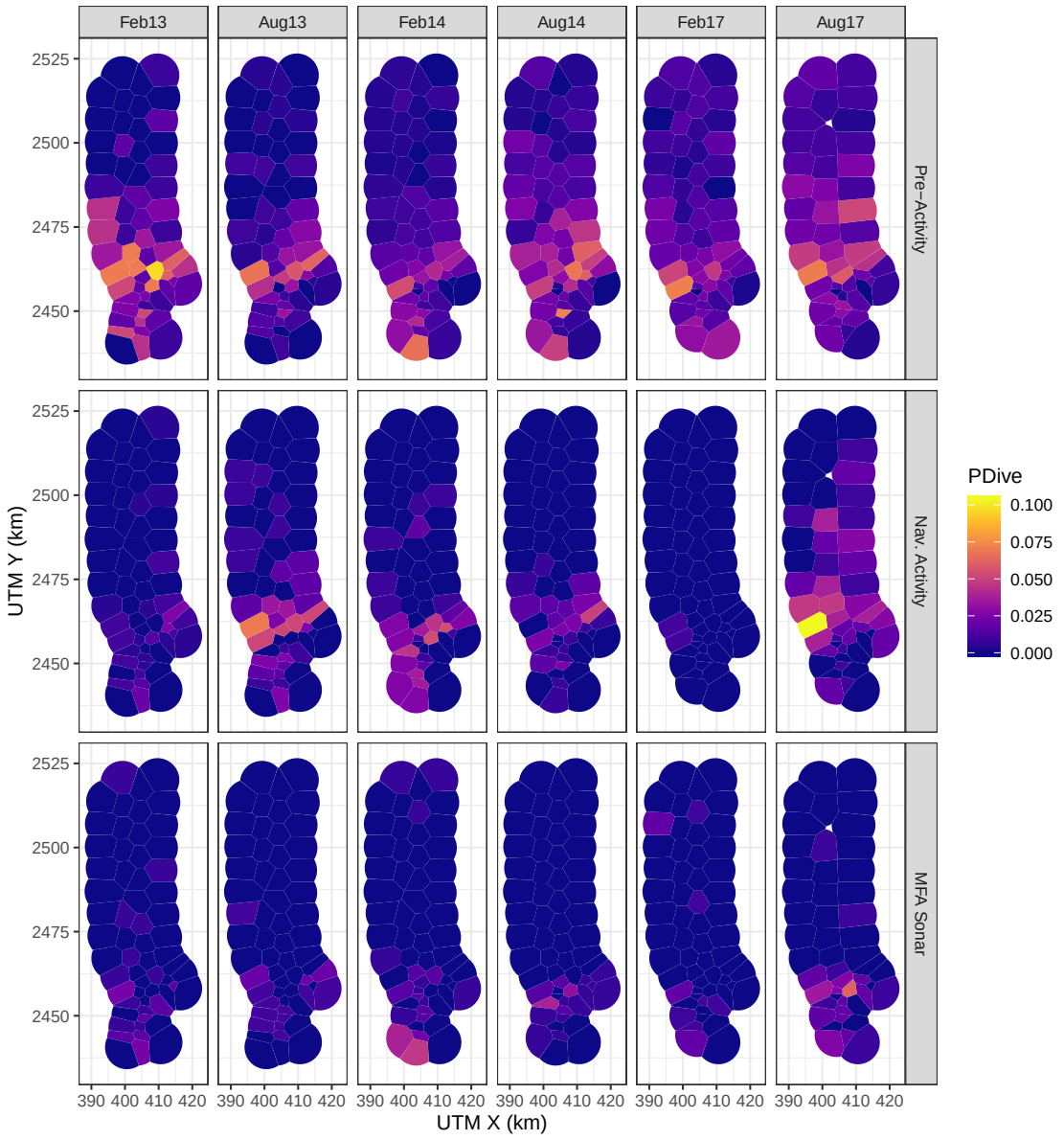

Figure 4: Map of observed probability of diving at each hydrophone before, during Phase A, and during Phase B of each SCC. Note that values of PDive are not corrected for effort (size of the hydrophone tile).

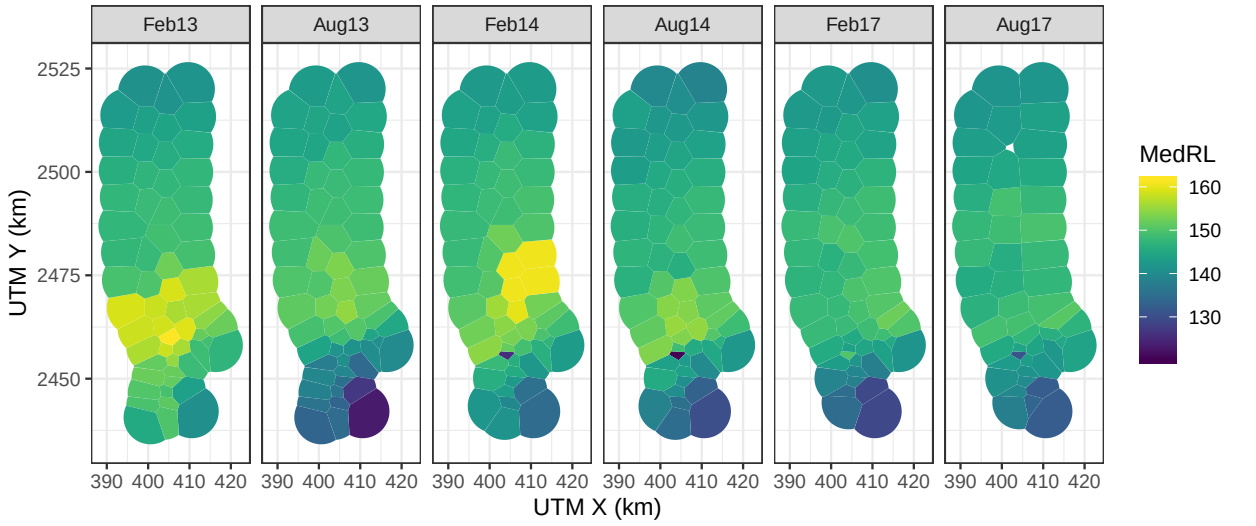

Figure 5: Median received level when MFA sonar was present (color scale) for all hydrophones and SCCs.